Proceedings of the 4th WSEAS Int. Conf. on HEAT TRANSFER, THERMAL ENGINEERING and ENVIRONMENT, Elounda, Greece, August 21-23, 2006 (pp83-88)

CFD modeling of the swirl-stabilised flame produced by a laboratory-scale combustor: selection of the turbulence model

[1*]A. HATZIAPOSTOLOU, [2]N.G. ORFANOUDAKIS, [2]M.K. KOUKOU,
[1]G. RAPTIS
[1]Energy Technology Dept., TEI of Athens, Ag. Spyridonos str., 12210, Athens, GREECE
[2]Mechanical Engineering Dept., TEI of Chalkida, 344 00 Psachna, Evia GREECE

Abstract: - A multi-fuel swirl-stabilized laboratory burner of 100kW total thermal input has been developed, designed as a scale model of a 110MW coal burner. This paper presents a computational investigation of the combusting flow field produced by the laboratory burner under varying aerodynamic conditions. The numerical predictions were compared with measured quantities in terms of velocities and temperatures at various distances away from the burner exit. Three turbulence models were tested, while for the combustion modeling, the non-premixed approach incorporating the mixture-fraction concept was employed. Satisfactory agreement between measured and predicted quantities was achieved, especially by applying the RNG k-ε and the Realizable k-ε turbulence models.

Key-Words: - combustion, swirl, laboratory-scale, simulation, turbulence

1 Introduction

Reduction of pollutant emissions and flame stabilization are important problems in combined cycle and conventional power plants. It is a common concern for combustor manufacturers and plant operators to achieve a reduction of the power plants' environmental effects, without a significant decrease in their efficiency, because of the recent European Directives [1-3]. An important way of understanding flame processes is to scale-up the measurements' results of tests on small burners to larger ones. Ideally, the result of a burner and flame scaling would be the complete similarity of all the combustion processes (turbulent transport and mixing, heat generation, heat transfer) in the scale down domain. However, that is not feasible, as all the physical and chemical processes will not scale down in the same way.

Towards the above issues, a multi-fuel swirl-stabilized laboratory burner of 100kW total thermal input has been developed, designed as a scale model of a 110MW coal burner. Constant velocity scaling criterion was applied to retain similarity to the industrial burner. Swirl in the burner air inlet stream is routinely used to achieve the desired ignition and burnout characteristics for a given fuel and to stabilise the flame. The laboratory burner is able to produce flames with different aerodynamic characteristics and to burn a combination of gaseous, liquid and pulverized solid fuels. In this context, the conditions for safe combustion of a combination of fuels in terms of flame stabilization, sufficient combustion efficiency and reduced pollutants emissions can be studied.

To enhance understanding on the effect of the swirl number on the fluid motion, the combusting flow field downstream the burner was investigated by the use of CFD techniques. Results are reported for two different swirl numbers and compared to experimental data obtained in the same burner.

2 Mathematical Formulation

2.1 The physical problem

Fig. 1 depicts the installation of the laboratory burner. The laboratory burner, which is shown schematically in Fig. 2, was designed as a scale model of an industrial coal burner operating in a cement rotary kiln. It can burn a mixture of liquid, gaseous and pulverized solid fuel simultaneously (if required) and produce flows with different degrees of swirl. Another basic design criterion was the similarity to the real industrial burner, which was accomplished by employing the constant velocity (CV) scaling criterion mentioned in [4]. The burner consists of a cylindrical body for the secondary airflow with a central fuel pipe. The exit of the burner is at the top of the burner and the diameter of the inner wall of the outer tube (shown as D_e) is known as the burner exit diameter. The latter is a characteristic dimension for every burner and in this case is D_e=64.5 mm. Secondary air is divided in swirl and axial air: the former is introduced tangentially from four entries located symmetrically around the burner, while the latter is introduced vertically to the outer wall of the burner from four

other entries located also symmetrically (Fig. 1.c). The axial flow has only axial velocity and the swirl flow has axial and tangential velocity components.

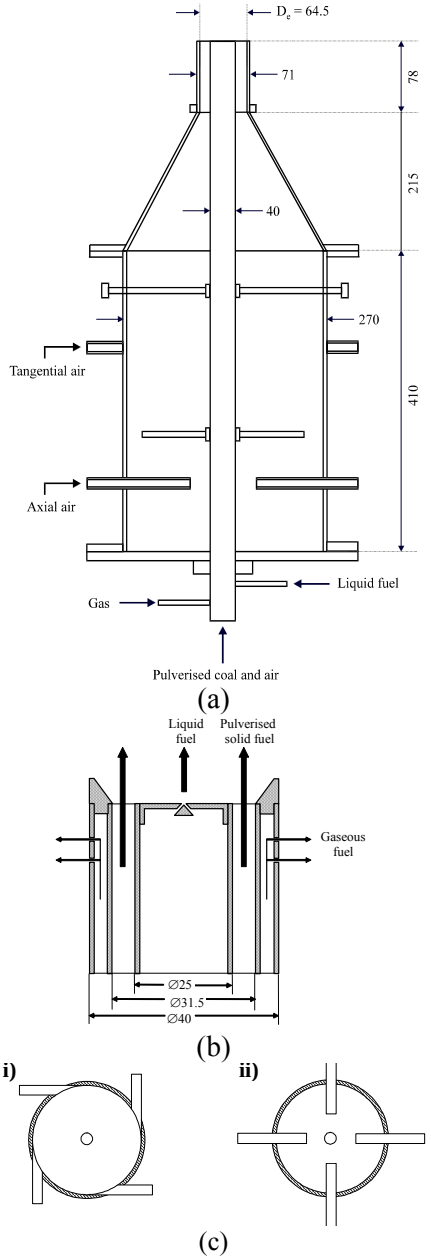

Fig. 1. Schematic of the laboratory burner (a) with detailed views of the fuel central pipe (b) and the inlets for tangential (c-i) and axial (c-ii) air.

At the upper part of the burner, the outer cylinder wall contracts to produce a homogeneous symmetrical secondary airflow at the burner exit. The central fuel pipe consists of three individually sealed coaxial tubes. The inner tube is for the liquid fuel, the annular area between the inner and the middle tube is for the pulverised coal and the annular area between the outer and the middle tube is for the gas fuel. The liquid fuel is dispersed at the end of the tube by an atomising nozzle. The pulverised coal is pneumatically conveyed by an airflow and is axially injected into the gas fuel flame as primary air/coal flow. The gas fuel is injected radially through two rows of 20 holes of 1mm diameter around the outer tube. The amount of swirl in the flow can be adjusted by varying the ratio of axial and tangential air, while maintaining the same total air flow rate.

2.2 Mathematical model

2.2.1 Computational mesh development

The simulations were performed for a flow domain that extended from the burner exit upwards at a distance of $20D_e$ and radially outwards at $7.5D_e$.

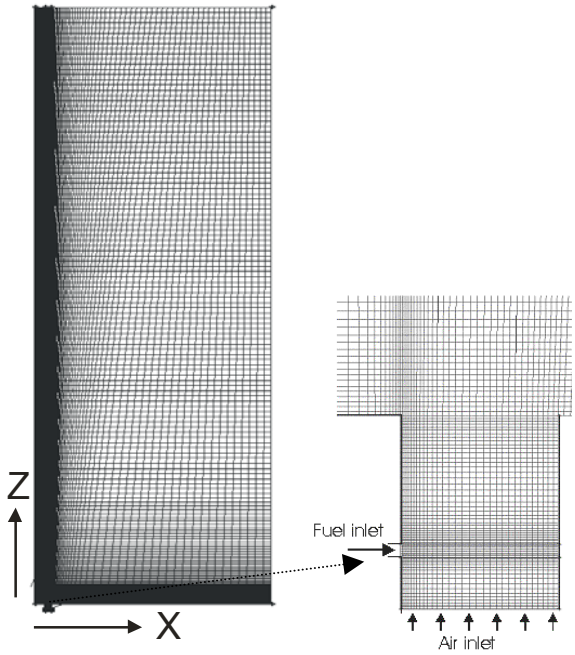

Fig. 2 View of the 2D mesh (Z symmetry axis) with enlarged detail of the fuel and air inlets.

Since the geometry is axisymmetric, the mesh covered half the domain to be solved (Fig.2). In order to employ the non-premixed modeling approach, the domain was extended 10mm inside the laboratory burner annulus, to incorporate the separate inlets for the fuel (see detail in Fig.2). A number of meshes with different densities were constructed in order to test the sensitivity of the solution. The mesh shown in Figure 2 was finally selected to be used in the simulations and consisted of 20344 cells.

2.2.2 Governing Equations - Boundary conditions

The turbulent flow field downstream the burner, was calculated from the solution of the two-dimensional, axisymmetric, steady-state, Reynolds-averaged Navier-Stokes equations by use of the commercially

available code Fluent®. As the non-premixed combustion scheme has been employed in the present study, the thermochemistry was reduced to a single parameter: the mixture fraction, which is defined as the mass fraction that originates from the fuel stream and is a conserved scalar quantity written in terms of the atomic mass fraction as:

$$f = \frac{Z_i - Z_{i,ox}}{Z_{i,fuel} - Z_{i,ox}} \qquad [1]$$

where Z_i is the elemental mass fraction for element, i. The subscript ox denotes the value at the oxidizer stream inlet and the subscript fuel denotes the value at the fuel stream inlet. This approach involves the solution of transport equation for the mixture fraction. Equations for individual species are not solved. Instead, species concentrations are derived from the predicted mixture fraction fields.

The axial and swirl air velocity profiles measured at an axial distance of 4.5mm away from the burner exit were transferred 14.5mm upstream and were used as boundary conditions in the calculations; the latter is expected to introduce minor errors in the predicted results. Methane and air enter the combustor in distinct streams, as shown in the detail of Fig. 2. Two cases corresponding to swirl numbers of 0.65 (low swirl) and 0.9 (high swirl) were considered.

2.2.3 Turbulence modeling

The Reynolds stresses which appear as unknowns in the Reynolds averaged forms of the Navier-Stokes equations for the velocity components were modeled by use of three turbulence models available in the Fluent® code: the standard k-ε model, the RNG k-ε model, based on the so-called "renormalization group theory", and the Realizable k-ε model. The standard two-equation k-ε turbulence model involves the solution of two additional partial differential equations for the turbulent kinetic energy (k) and its dissipation rate (ε) [7,8]. The values of the constants C_μ, C_1, C_2, σ_κ and σ_ε applied are 0.09, 1.44, 1.92, 1.0 and 1.3 respectively [7,8]. The RNG k-ε model is essentially a variation of the standard k-ε model, with the used constants estimated rather through a statistical mechanics approach than from experimental data. The values of the constants C_μ, C_1 and C_2 applied are 0.0845, 1.42 and 1.68, respectively [9]. The Realizable k-ε model contains a new formulation for the turbulent viscosity. Also, a new transport equation for the dissipation rate, ε, has been derived from an exact equation for the transport of the mean-square vorticity fluctuation [10]. Both the Realizable and RNG k-ε models have shown substantial improvements over the standard k-ε model where the flow features include strong streamline curvature, vortices and rotation. Since the last model is still relatively new, it is not clear in exactly which instances the Realizable k-ε model consistently outperforms the RNG model. The accuracy of the predictions of these models was checked against the measured flow field (swirl and axial velocities).

2.2.4 Combustion modeling

The non-premixed combustion scheme employed in the present study, was based on the assumption of equal diffusivities for all species, which is generally acceptable for turbulent flows such as the one under investigation. The main parameter which was used in the calculations was the mixture fraction. As the diffusion coefficients for all species are equal, Eq. [1] is identical for all elements, the mixture fraction definition is unique and it is thus the elemental mass fraction that originates from the fuel stream. Under the assumption of chemical equilibrium, combustion can be simplified to a mixing problem and the turbulence-chemistry interaction is accounted for with a Probability Density Function having a β-function shape, which most closely represents experimentally observed PDFs [10]. Thermo-chemistry was pre-computed and a look-up table was generated, containing mean values of species fractions, density and temperature as a function of mean mixture fraction and mean mixture fraction variance. This look-up table provided the closure model during the reacting flow calculations performed at a later stage.

2.2.5 Numerical solution details

The solution of the set of the equations has been made with the segregated steady-state solver [10] embodied in the Fluent® commercial software. The convergence is checked by several criteria (e.g. the conservation equations should be balanced; the residuals of the discretised conservation equations must steadily decrease).

3 Results and Discussion

Detailed velocity and temperature data were obtained by means of a one-component LDV (laser Doppler velocimetry) system and a 250 μm diameter Pt/Pt10%Rh thermocouple [11]. The present investigation is the continuation of a recent research work [12], where predicted results for the non-reacting flow field were compared with the equivalent experimental data.

Figs. 3 to 6 present radial half profiles of the mean swirl and axial velocity components for the two flow

axes with different swirl numbers at two different distances from the burner exit. All radial profiles shown are halves, with the axis of symmetry at x=0. The graphs show the measured values along with the computed results using the three turbulence models mentioned in 2.2.3.

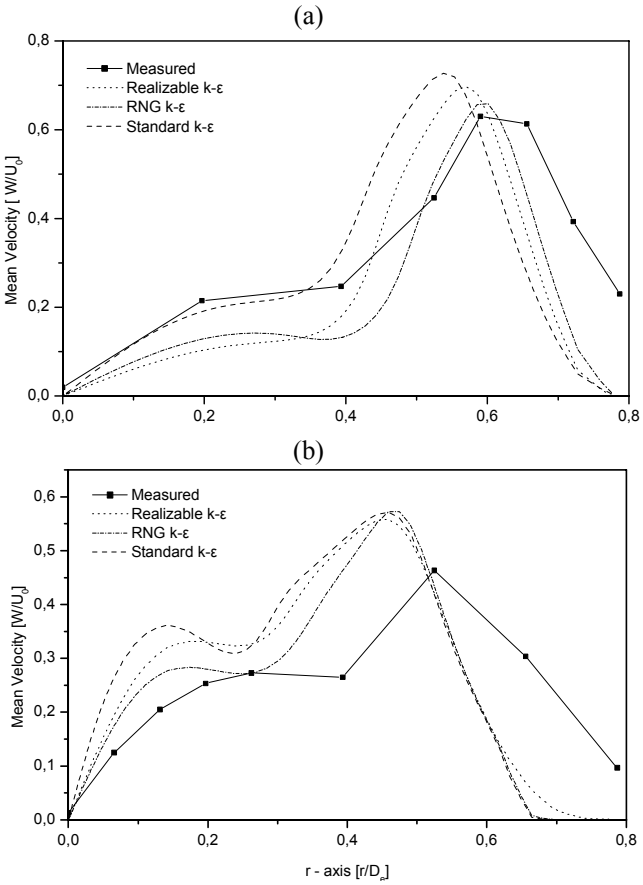

Fig. 3. Radial (half) profiles of the mean swirl velocity component for the two reacting flow cases (a) S_w=0.65 at z/D_e=0.78 and (b) S_w=0.90 at z/D_e=0.62

In general the calculations tend to predict correctly the profile shapes with variable success, as far as the measured values are concerned. At the near-burner region all models tend to over-predict mean velocity component values by approximately 15-30% compared to the measured ones (Figs. 3,4). It is also evident that the standard k-ε model tends to produce inferior results than the other two turbulence models, which is in agreement with the conclusions of a previous study [12]. For the case of S_w = 0.65 and at a distance of 0.78De from the burner exit (Fig. 3a), the application of the RNG k-ε model gives the most satisfactory results for the swirl velocity component. However, all turbulence models give similar results for the case of S_w=0.90 (Fig. 3b). Figs. 4a,b depicts the axial velocity components at the same locations, where the radial extent of the internal recirculation zone (IRZ) can be noticed. Higher swirl is associated with a larger IRZ, which, in turn, plays an important role in the flame stabilization [4,6].

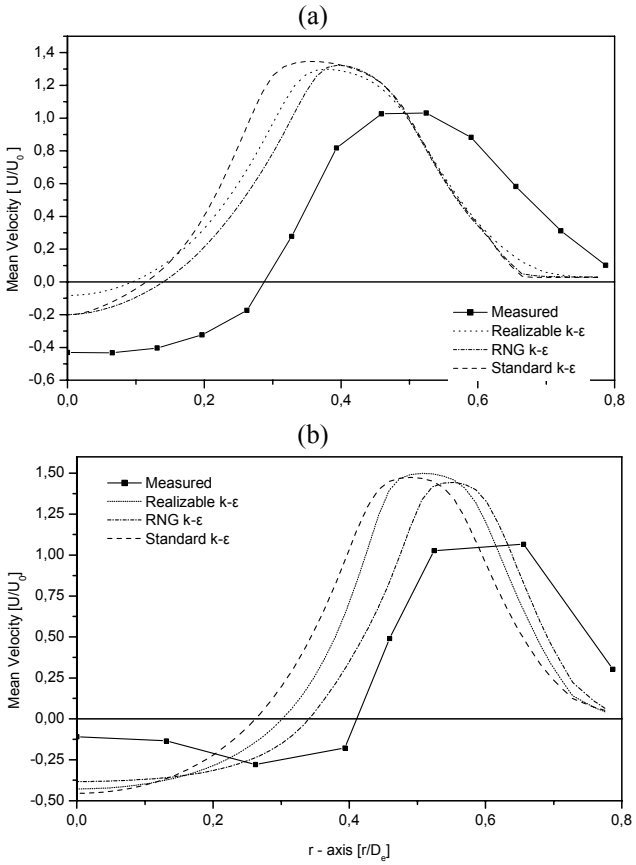

Fig. 4. Radial (half) profiles of the mean axial velocity for the two reacting flow cases (a) S_w=0.65 at z/D_e=0.78 and (b) S_w=0.90 at z/D_e=0.62

For both swirl number cases, it can be deduced that calculations predict qualitatively the existence of the IRZ, however, the application of the RNG k-ε gives more realistic results in quantitative terms.

The radial velocity components were also measured at the same axial locations, but they are not shown, as their magnitude is considerably smaller and, most importantly, their radial profiles tend to strongly deviate from the axial symmetry, possibly due to minor burner structural asymmetries.

In Figs. 5 and 6 similar profiles far from the burner exit ($z = 3.1D_e$ or $3.57D_e$) for the two swirl numbers examined are shown. The computed swirl velocity components by means of all turbulence models, agree very well with the measured ones. A small advantage of the RNG k-ε model can be still deduced from Fig.5b. The axial velocity components at these axial locations do not have negative values at all radial distances, as the IRZ effect does not extend so far from the burner exit. For S_w=0.65 calculated values by applying the RNG k-ε model have an excellent agreement with the measured values close to the inlet, however, there is a

discrepancy far away from it. For S_w=0.90 all the turbulence models over predict the measured values although their trend is correctly predicted.

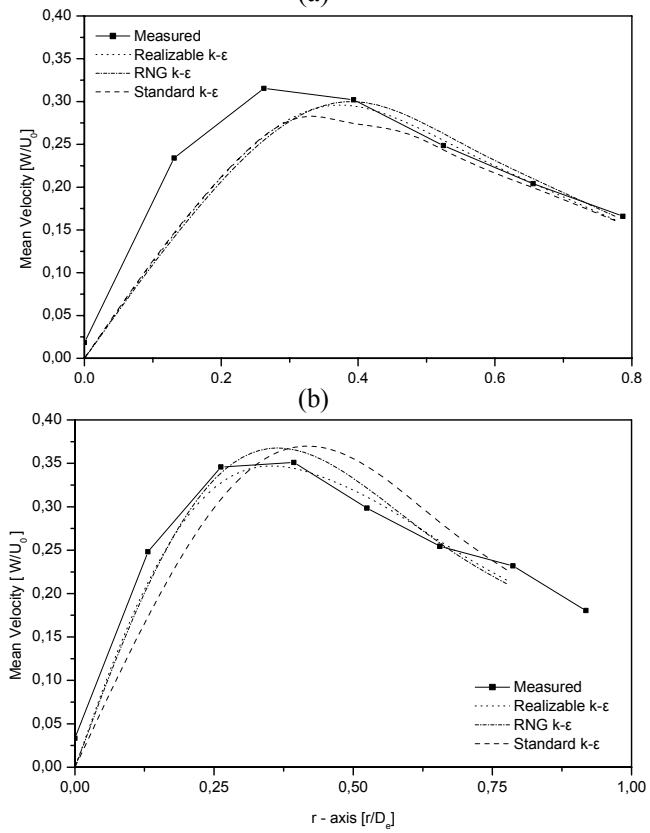

Fig. 5. Radial (half) profiles of the mean swirl velocity component for the two reacting flow cases (a) S_w=0.65 at z/D_e=3.1 and (b) S_w=0.90 at z/D_e=3.57

Fig. 7 shows radial profiles of the mean temperature close to the burner exit. The comparison between computed and measured values shows good qualitative agreement in predicting the "hot" areas around the axis of symmetry. However, in quantitative terms, there is a 30% underestimation by all turbulence models, in the case of S_w=0.65 and a 5-20% overestimation, in the case of S_w=0.90.

Finally, results from the most successful turbulence model, the RNG k-ε, are shown in Fig 8, in the form of full flow fields with pathlines. The whole domain is not shown instead the near-burner region was selected to be depicted for both swirl number cases. A mirror image of the computed half-domain was added, in order to visualize better the phenomena. Fig. 8a presents the flow field for the S_w=0.65 case, where the maximum dimensions of the IRZ are approx. $1D_e$ along the centerline and $0.48D_e$ (or $\pm 0.24D_e$) radially. The IRZ for the S_w=0.90 case extends $2.6D_e$ along the centerline and is almost 100% wider than in the previous case ($\pm 0.43D_e$).

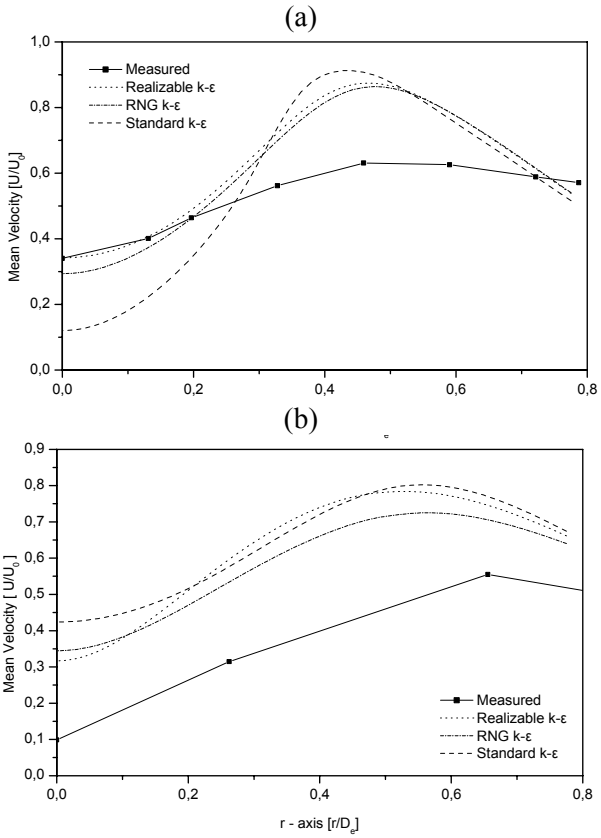

Fig. 6. Radial (half) profiles of the mean axial velocity for the two flow cases (a) S_w=0.65 at z/D_e=3.1 and (b) S_w=0.90 at z/D_e=3.57

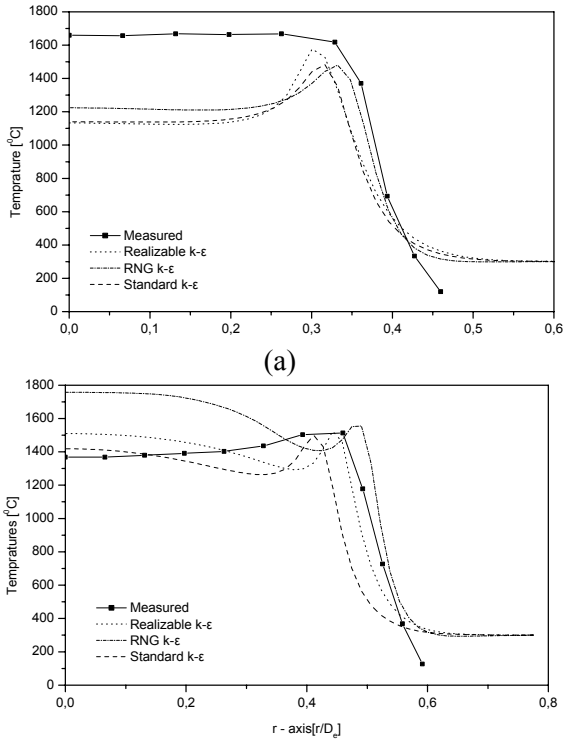

Fig. 7. Radial (half) profiles of the mean temperature for the two reacting flow cases (a) S_w=0.65 at z/D_e=0.78 and (b) S_w=0.90 at z/D_e=0.62

These results quantify the effect of variable swirl in these combusting flows and can be used in order to design combustor geometries with improved performance.

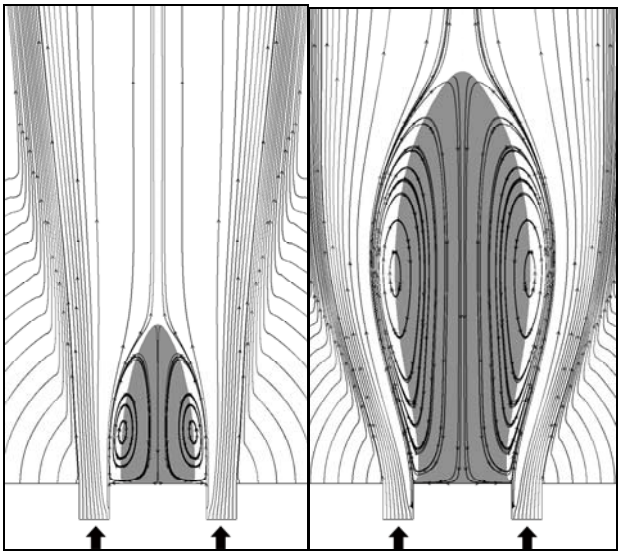

Fig. 8. Computed near-burner full flowfields by means of the RNG *k-ε* model showing pathlines and the IRZ (grey-shaded areas) for the two reacting flow cases (a) S_w=0.65 and (b) S_w=0.90

4 Conclusion

A CFD model has been used to predict the combusting flow field produced by a multi-fuel swirl-stabilized laboratory burner with adjustable aerodynamics, which was designed as a scale model of an industrial coal burner. Results are reported for two different swirl numbers and compared to measured velocity and temperature data. The non-premixed combustion scheme involving the mixture fraction approach has been employed and the turbulence-chemistry interaction was accounted for with a Probability Density Function having a *β*-function shape. For the description of turbulence, three turbulence models were tested, the standard k-ε model, the RNG k-ε model and the Realizable k-ε model. In general the calculations tend to predict correctly the experimental profile shapes. For both swirl number cases, the application of the RNG k-ε and Realizable k-ε turbulence models gives more realistic results in quantitative terms, with the RNG k-ε having a small advantage.

5 Acknowledgement

This research work was co-funded by the European Social Fund and National resources (EPEAEK II) Archimedes I and II.

References:

[1]N.G. Orfanoudakis, K. Krallis, A. Hatziapostolou, A. Vakalis, N.W. Vlachakis, Emission Reduction Techniques: the IPPC EC Directive, Air Pollution 2004, Rhodes GREECE, WIT Press.

[2]W. Kaewboonsong, V.I. Kouprianov, Minimizing fuel and "external" costs for a variable-load utility boiler firing fuel oil", *Int. Journal of Thermal Sciences*, Vol. 42, 2004, pp. 889-895.

[3]G.L. Borman, K.W. Ragland, *Combustion Engineering*, Mc Graw Hill, New York, 1998.

[4]J.P. Smart, D..J. Morgan, The comparison between constant velocity and constant residence time scaling of the aerodynamically air staged burner, Netherlands: International Flame Research Foundation Doc No F37/y/28, 1992.

[5]N.G. Orfanoudakis, Measurements of size and velocity of burning coal, PhD Thesis, Imperial College of Science, Technology and Medicine, Department of Mechanical Engineering, 1994.

[6]A. Hatziapostolou, Swirling flows in direct-injection diesel engines, PhD Thesis, Imperial College of Science, Technology and Medicine, Department of Mechanical Engineering, 1991.

[7] B.E. Launder, D.B. Spalding, The Numerical Computation of Turbulent Flow, *Computer Methods in Applied Mechanics and Engineering*, Vol. 3, 1974, pp. 269-289.

[8] W. Rodi, *Turbulence models and their application in hydraulics – A state of the art review*, Int. Ass. for Hydraulics Research, 1980.

[9] V. Yakhot, S.A. Orszag, Renormalization group analysis of turbulence. I. Basic theory, *Journal of Scientific Computing*, Vol. 1 (1), 1986, pp. 3-51.

[10] Fluent® User's Guide.

[11] N. Orfanoudakis, A. Hatziapostolou, K. Krallis and N. Vlachakis. "Design and evaluation measurements of a swirl stabilised laboratory burner" *IMechE C20704, Journal of Mechanical Engineering Science - Part C*, Vol. 219, 2005, pp.1079-1086.

[12] A. Hatziapostolou, K.Krallis, N.G. Orfanoudakis, M.K.Koukou, D. Chatzifotis, G. Raptis, Numerical prediction of the flow field produced by a laboratory-scale combustor: a preliminary isothermal investigation, *WSEAS Transactions on Fluid Mechanics*, 3, Vol. 1, 2006, pp. 230-235.